Ultraviolet Irradiation of Nucleic Acids: Formation, Purification, and Solution Conformational Analyses of Oligothymidylates Containing Cis-Syn Photodimers†

Robert E. Rycyna,‡ John C. Wallace, Minoti Sharma, and James L. Alderfer*
Biophysics Department, Roswell Park Memorial Institute, Buffalo, New York 14263
Received July 20, 1987; Revised Manuscript Received December 14, 1987

ABSTRACT: Acetone-photosensitized UV irradiation of three thymine oligomers, d(TpT), d(TpTpT), and d(TpTpTpT), forms predominantly cis-syn cyclobutyl photodimers. C-18 reverse-phase high-performance liquid chromatography is used to purify the following positional isomers: d(TpT[p]T), d(T[p]TpT), d-(TpTpT[p]T), d(TpT[p]TpT), d(T[p]TpTpT), and d(T[p]TpT[p]T), where T[p]T represents the cis-syn photodimer. Conformational properties of the cis-syn dimers and adjacent thymine nucleotides have been investigated in solution by using ^{1}H, ^{13}C, and ^{31}P NMR spectroscopy. These studies show that (1) the photodimer conformation in longer oligothymidylates is similar to that in the dinucleoside monophosphate and (2) the cis-syn dimer induces alterations to a greater degree on the 5′ side than on the 3′ side of the photodimer. Specifically, the photodimer distorts the exocyclic bonds ϵ(C3′–O3′) in Tp- and γ(C5′–C4′) in -pT[p]- on the 5′ side and slightly alters the furanose equilibrium of the -pT nucleotide on the 3′ side of the dimer.

Ultraviolet (UV)[1] light is known to profoundly affect the structure, the conformation, and the biological activity of nucleic acids (Wang, 1976). The ability of nucleic acids to absorb light in the UV-B region (290–320 nm) of the solar spectrum provides the potential for the induction of photochemical alterations in macromolecules that encode information basic for cell survival. At least in simple systems, DNA has been shown to be the most important target for ultraviolet irradiation (Hutchinson, 1966; Setlow, 1966). The formation of a variety of UV photoproducts is known to interfere with cellular processes such as DNA replication (Bollum & Setlow, 1963; Radman et al., 1977; Chan et al., 1985), transcription (Sauerbier, 1976), and endonucleolytic cleavage (Setlow et al., 1964; Hall & Larcom, 1982). A more complete understanding of both the biological effects of radiation-induced damage to cells as well as perhaps factors responsible for photolesion recognition by repair enzymes will evolve through knowledge gained of the structural features of these altered nucleic acids.

An abundance of information has been obtained on the most predominant DNA photolesion, the cyclobutane-type pyrimidine photodimer (Fisher & Johns, 1976). This type of photoproduct is induced in DNA by irradiation with far- and near-UV light and has been implicated in UV-induced lethality, mutagenicity, and tumorigenicity (Hart et al., 1977; Rothman & Setlow, 1979; Suzuki et al., 1981). Stereochemically, cyclobutyl-linked pyrimidines may exist in six configurationally distinct orientations, the predominant one being the cis-syn isomer (Varghese, 1972). Previously, the disruptive influence of a photodimer on the local integrity of DNA structure has been examined in the most simple oligomer, the dinucleoside monophosphate. Significant conformational changes have been observed in d(TpT) through an extensive NMR study of the cis-syn d(TpT) photodimer, herein abbreviated d(T[p]T), by Hruska et al. (1975), Liu and Yang (1978), and Rycyna and Alderfer (1985). The crystallographic structure of this same d(T[p]T) dimer possessing a cyanoethyl phosphotriester linkage indicates some unexpected conformational changes associated with cis-syn cyclobutane ring formation (Cadet et al., 1985). The first step to understanding the distortion induced into the secondary structure of a DNA helix by such a photolesion is to examine the intrastrand effects on adjacent nucleotides.

In the present work, the conformational features of thymine nucleotides adjacent to a *cis-syn*-d(T[p]T) in solution are examined in three oligothymidylates, d(TpT), d(TpTpT), and d(TpTpTpT). Each thymine oligomer is subjected to acetone-photosensitized irradiation conditions which are known to form only photodimers (Greenstock & Johns, 1968; Kucan et al., 1972); purification of the photodimers occurs with C-18 reverse-phase high-performance liquid chromatography (HPLC). Solution conformational investigations of thymine oligomers containing cis-syn photodimers are done by using multinuclear NMR techniques. These studies reveal that the cis-syn dimer induces conformational alterations to a greater degree on the 5′ side than on the 3′ side of the photodimer. Specifically, the photodimer distorts the exocyclic bonds ϵ(C3′–O3′) in Tp- and γ(C5′–C4′) in -pT[p]- on the 5′ side of the dimer and slightly alters the furanose equilibrium of the -pT nucleotide on the 3′ side of the dimer. An independent study of the duplex d(GCGTTGCG)·d(CGCAACGC) containing a *cis-syn*-d(T[p]T), which was published by Kemmink et al. (1987) during the preparation of this paper, also cor-

† This work was supported by grants from the National Institutes of Health (CA39027 and 2T32-ES07057). Some of the NMR measurements were performed on an instrument purchased through grants from the Division of Research Resources of the NIH and from the Biophysics Program of the National Science Foundation. We acknowledge the financial support (to R.E.R.) of the SUNY/Buffalo Graduate Student Association.

* Author to whom correspondence should be addressed.
‡ Present address: Chemistry Department, Yale University, New Haven, CT 06511.

[1] Abbreviations: UV, ultraviolet; NMR, nuclear magnetic resonance; d(T[p]T), cis-syn cyclobutane-type photodimers of d(TpT); DpT and TpD, trimer positional isomers of d(T[p]TpT) and d(TpT[p]T), respectively; DpTpT, TpDpT, etc., tetramers d(T[p]TpTpT), d(TpT[p]-TpT), etc., containing photodimers; NOE, nuclear Overhauser effect; COSY, two-dimensional scalar-correlated spectroscopy; EDTA, ethylenediaminetetraacetic acid; TBA, *tert*-butyl alcohol; TMP, trimethyl phosphate; TSP, sodium 3-(trimethylsilyl)[2,2,3,3-^{2}H]propionate.

0006-2960/88/0427-3152$01.50/0

roborated, although in a qualitative sense, the differential distortion on the 5′ and 3′ sides of the photodimers.

Materials and Methods

Materials. d(TpT) and d(TpTpT) were synthesized by using the phosphotriester approach by J.C.W. $d(Tp)_4$ was also synthesized through the phosphotriester approach by M.S. and the terminal 3′-phosphate removed by bacterial alkaline phosphatase. 99.96% D_2O was obtained from Bio-Rad Laboratories.

UV Irradiation Source. Four Westinghouse sunlamps (FS20T12) emitting a power spectrum of 310 ± 35 nm were used for sensitized irradiations.

Acetone-Photosensitized Irradiation. Each thymine oligomer, 50 mg of d(TpT), 42 mg of d(TpTpT), and 120 mg of d(TpTpTpT), was diluted separately to a concentration of 1 mM in 5% aqueous acetone and transferred to Pyrex Petri dishes (9-cm diameter). These solutions were irradiated with a UV fluence of 3.0 J/(m^2·s) under a nitrogen atmosphere. Measurement of UV fluence is done by using a long-wavelength Blak-Ray ultraviolet meter from UV Productions. Samples are maintained at 2 °C by placing Petri dishes on a $^1/_4$-in. aluminum plate, which is temperature controlled by a circulating coolant. Product formation was monitored periodically by ^{31}P NMR spectroscopy. During extended irradiations, a volume of acetone equal to that initially mixed was added every 2 h to replace the acetone lost due to evaporation. UV irradiation continued until the samples received the following doses: d(TpT), 150 kJ/m^2; d(TpTpT), 225 kJ/m^2; and d(TpTpTpT), 250 kJ/m^2. Aqueous acetone was removed immediately by flash evaporation and the irradiated oligomer resuspended in a minimum volume of appropriate solvent for subsequent HPLC separation.

Chromatography of Thymine Oligomer Photoproducts. (A) d(TpT) Photoproducts. UV-irradiated d(TpT) (25 mg) was twice injected onto a 5-μm Ultrasphere (10 mm × 25 cm) semipreparative C-18 reverse-phase column and eluted with a linear gradient of 180 mL of 75 mM KH_2PO_4 (pH 4.5) to 180 mL of 40% (v/v) MeOH/75 mM KH_2PO_4 (pH 4.5) at 4 mL/min. Separated photoproducts were reinjected onto the column and desalted with a 60 mL of H_2O to 60 mL of 50% MeOH/H_2O gradient.

(B) d(TpTpT) Photoproducts. The procedure is the same as described for d(TpT) with the exception that only 21 mg of UV-irradiated d(TpTpT) was twice injected onto the column.

(C) d(TpTpTpT) Photoproducts. UV-irradiated d(TpTpTpT) (120 mg) was loated onto a 5-μm Zorbax (21 mm × 25 cm) preparative C-18 reverse-phase column by Dupont and eluted at 8 mL/min with a linear gradient of 425 mL of 100 mM KH_2PO_4 (pH 4.5) to 425 mL of 50% (v/v) MeOH/100 mM KH_2PO_4 (pH 4.5). The separated photoproducts were reinjected onto a 5-μm Ultrasphere (10 mm × 25 cm) C-18 reverse-phase column and desalted by using a 60 mL of H_2O to 60 mL of 50% (v/v) MeOH/H_2O gradient at 4 mL/min.

NMR: Sample Preparation. ^{31}P NMR samples (10-mm tubes) were dissolved into 1.3 mL of 40% D_2O containing 4 mM EDTA (pH 7.0) and 10 mM TMP [used as internal chemical shift reference where δ(85% H_3PO_4) = δ(TMP) + 3.71 ppm]. Typical concentrations of oligomers for phosphorus NMR analysis were 2.5 mM tetramers, 10 mM trimers, and 16 mM d(T[p]T). ^{13}C NMR samples (in 5-mm tubes) were prepared in a similar fashion with the exceptions that dioxane was the internal reference and the final volume was 0.4 mL. Sample concentrations for ^{13}C NMR studies were about 10 mM for tetramers, 35 mM for trimers, and 50 mM for d(T[p]T). ^1H NMR samples were lyophilized 2 times from 99.8% D_2O, dissolved into 0.35 mL of 99.96% D_2O containing either 60 mM d(T[p]T), 50 mM DpT or TpD, or 15 mM tetramer photoproducts and 0.5 mM EDTA (pH 7.38), 5 mM NaH_2PO_4 (pH 7.4), and 10 mM TBA, and transferred into 5-mm tubes. Proton chemical shift values are reported relative to internal TSP where δ(TSP) = δ(TBA) + 1.2542 ppm at 30 °C. The pH_{obsd} is the pH meter reading of D_2O solutions. Unless specifically mentioned, all ^1H, ^{13}C, and ^{31}P chemical shift values are reported at 30 °C.

NMR: Conventional Acquisitions. ^{31}P NMR data were recorded by a Bruker WP-200 (80.961 MHz) operating in the pulsed Fourier transform (FT)/quadrature phase acquisition mode. Field stabilization was maintained by internal locking to the deuterium resonance of the solvent. Free-induction decay (FID) data were accumulated and transformed by an Aspect 2000 minicomputer. ^{31}P spectra were recorded after using an inverse-gated routine [proton decoupled without nuclear Overhauser effect (NOE)] or a gated sequence (proton coupled with NOE). ^{13}C NMR spectra were recorded by a Bruker AM-400 (100.621 MHz) using broad-band proton decoupling. ^1H NMR data were acquired on our own Bruker AM-400 (400.135 MHz), a Bruker AM-500 (500.138 MHz) at Bruker Spectrospin, Ltd. (Canada), the WP-500 (500.136-MHz) spectrometer at the Chemical Instrumentation Center, Yale University, and the 600-MHz spectrometer at the NMR Facility for Biomedical Studies (Carnegie-Mellon Institute).

NMR: Two-Dimensional (2-D) COSY Acquisitions. A pulse sequence 90°–t_1–90°–FID(t_2) was used. 2-D COSY data sets consisted of 512 data points along t_1 and 2048 points along t_2 with spectral widths of 950 and 1900 Hz, respectively. Digital resolution was 1.85 Hz/point along t_1 and 0.925 Hz/point along t_2. A total of 16 transients were accumulated for each value of t_1 with a 2.0-s delay between observation pulses. A 16-step phase-cycling procedure for quadrature detection suppressed phantom peaks. Data matrix was zero-filled to 1024 points along t_1, both dimensions were multiplied by a sine bell function, and after 2-D transformation, the data were symmetrized.

Spectral Simulations. All ^1H NMR parameters for d(TpTpT) and cis-syn photodimers of d(TpTpT) listed in Table III as well as some parameters for d(TpTpTpT) and *cis-syn*-d(TpT[p]TpT) listed in Table IV were refined by using the iterative spin-simulation program PANIC.[2] Simulations were performed on proton NMR data obtained both at 500 MHz and at 600 MHz. The calculated errors of the parameters were usually between 0.09 and 0.12 Hz for 600–800 transitions. After individually simulated furanose and base proton spin systems of the trimer models received an appropriate line-broadening treatment, they were added together in order to obtain a complete proton spectrum of the molecule.

Results

Photoproduct Formation and Positional Assignment. Since sensitized UV irradiation of d(TpT) is known to form almost exclusively the cis-syn photodimer (Rycyna & Alderfer, 1985), a preponderance of photodimers possessing the same configuration is expected to form in longer thymine oligomers, d-

[2] PANIC (Parameter Adjustment in NMR by Iterative Calculation) is a minicomputer version of the LAOCOON-type programs, provided in the software packages of the Bruker NMR spectrometers by Bruker Instruments, Inc., Billerica, MA.

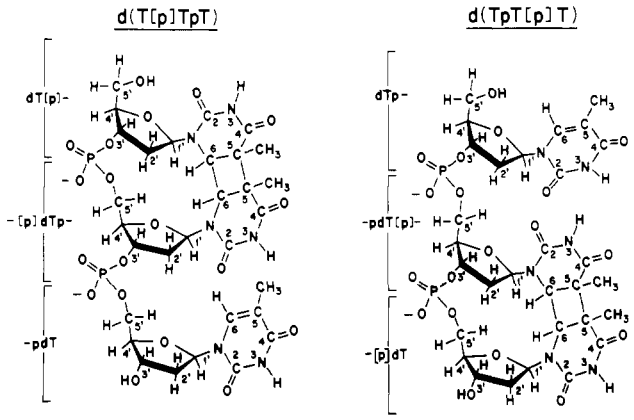

FIGURE 1: Structural formula of d(T[p]TpT), abbreviated as DpT (left), and d(TpT[p]T), abbreviated as TpD (right).

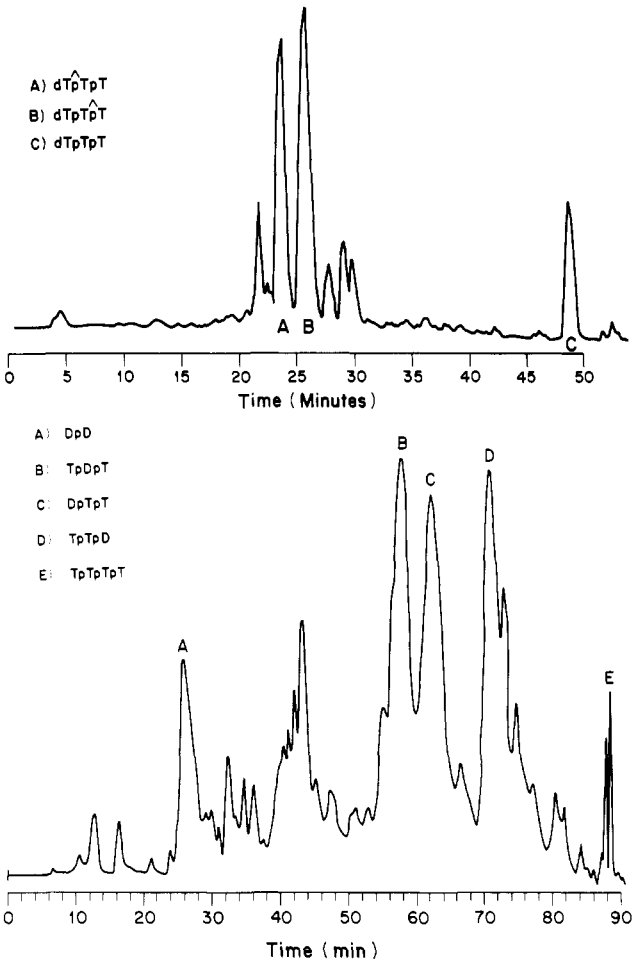

FIGURE 2: Preparative C-18 reverse-phase HPLC profiles of photoproducts from photosensitized UV irradiation of d(TpTpT) (top) and d(TpTpTpT) (bottom).

(TpTpT) and d(TpTpTpT), with similar irradiation conditions. Thymine bases in these three oligomers may be photochemically joined at the 5,6 bonds, yielding many positional isomers such as d(T[p]T), d(TpT[p]T), d(T[p]TpT), d(TpTpT[p]T), d(TpT[p]TpT), d(T[p]TpTpT), and d(T[p]TpT[p]T), where T[p]T represents cyclobutyl-linked thymines. Structural formulas of trimer positional isomers d(TpT[p]T) (hereafter abbreviated TpD) and d(T[p]TpT) (abbreviated DpT) are shown in Figure 1. Addition of single thymine nucleotides onto either end enables the construction of structural formulas of tetramers containing photodimers, which are abbreviated as TpTpD, TpDpT, and DpTpT.

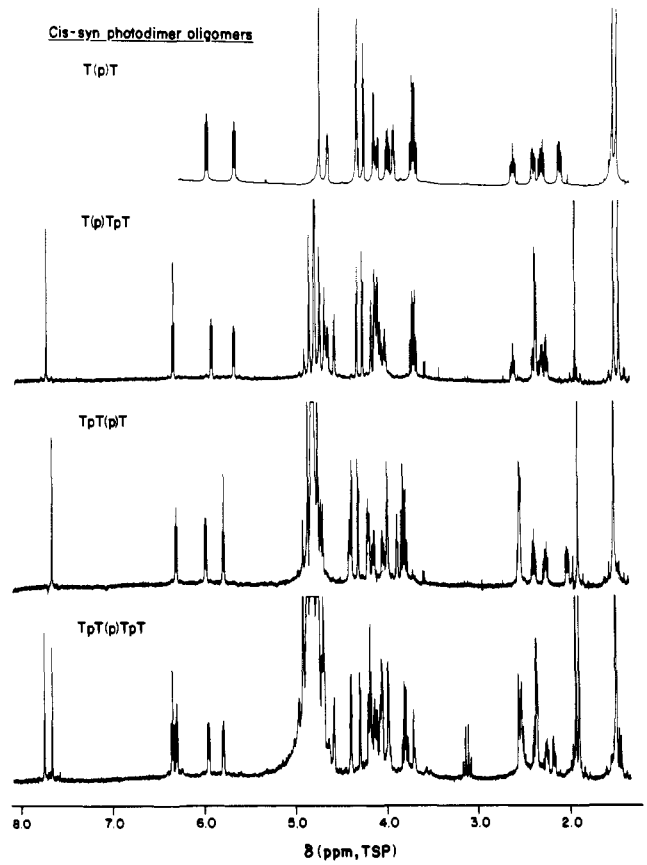

FIGURE 3: ^{1}H NMR spectra at 30 °C in D_2O of cis-syn photodimers of d(T[p]T) at 500 MHz and d(T[p]TpT), d(TpT[p]T), and d-(TpT[p]TpT) at 600 MHz.

Two oligothymidylates [d(TpTpT) and d(TpTpTpT)] have been exposed to acetone photosensitization conditions as described under Materials and Methods and their photoproducts separated as shown in Figure 2 by using HPLC. Three major trimer fractions and five predominant tetramer fractions containing various photoproducts were collected. It is obvious that numerous other products are formed during the irradiation process; many of these represent photodimers possessing different cyclobutane configurations in a variety of positions. The approach used to identify the cyclobutane ring configuration in these HPLC fractions begins at the dimer level, d(TpT), since a complete phosphorus (Rycyna & Alderfer, 1985) and proton (Hruska et al., 1975) resonance assignment has been made of the *cis-syn*-d(T[p]T) photodimer. First, ^{31}P NMR spectroscopy was used to obtain simple information about the oligomer photoproducts based on the sensitivity of the phosphorus chemical shift to torsion angles α(P–O5′) and ζ(O3′–P) and the O–P–O bond angle (Gorenstein, 1978). The ^{31}P resonance of the internal phosphodiester (-[p]-) shifts upfield about 0.5 ppm to −4.52 ppm due to formation of the cis-syn cyclobutane ring (Rycyna & Alderfer, 1985). Phosphorus chemical shift positions in the oligomers containing photodimers reported in Table I also show a resonance shifted far upfield to the same region (−4.40 to −4.60 ppm), indicating the likelihood of cis-syn cyclobutyl-linked bases. Therefore, phosphorus NMR data suggest the formation and isolation of oligomers containing the cis-syn photodimer. Proton NMR was definitive in confirming the presence of the cis-syn isomer in the trimers and tetramers. Figure 3 shows the ^{1}H NMR spectra of *cis-syn*-d(T[p]T) (top), trimer fractions A (second from top) and B (second from bottom), and tetramer fraction B (bottom). The presence in the trimers of the AB spin system at 4.25–4.35 ppm (assigned as H6 protons) along with a J_{66}

Table I: ^{31}P NMR Chemical Shift Values[a] of Cis-Syn Photodimers[b] in Thymine Oligomers

HPLC fraction[c]	oligomer	assigned phosphorus	18 °C	30 °C	63 °C	$\Delta\delta$[d]	$\Delta\Delta\delta$[e]
	d(TpT)	TpT	−4.072	−4.010	−3.828	0.244	n/a[f]
	d(T[p]T)	T[p]T	−4.563	−4.517	−4.367	0.196	−0.491
C	d(TpTpT)		−4.185	−4.124	−3.964	0.221	n/a
			−4.198	−4.136	−3.970	0.228	n/a
B	d(TpT[p]T)	Tp-	−3.879	−3.848	−3.728	0.151	+0.306
		-T[p]T	−4.482	−4.468	−4.403	0.079	−0.284
A	d(T[p]TpT)	T[p]T-	−4.627	−4.574	−4.418	0.209	−0.442
		-pT	−4.120	−4.058	−3.884	0.236	+0.078
E	d(TpTpTpT)		−4.182	−4.132	−3.972	0.210	n/a
		-TpT-	−4.268	−4.214	−4.052	0.216	n/a
			−4.205	−4.149	−3.984	0.221	n/a
D	d(TpTpT[p]T)	Tp-	−4.220	−4.162	−3.994	0.226	−0.038
		-TpT-	−3.948	−3.917	−3.809	0.139	+0.320
		-T[p]T	−4.468	−4.455	−4.407	0.061	−0.263
B	d(TpT[p]TpT)	Tp-	−3.879	−3.845	−3.726	0.153	+0.303
		-T[p]T-	−4.624	−4.595	−4.498	0.126	−0.356
		-pT	−4.169	−4.106	−3.927	0.242	+0.036
C	d(T[p]TpTpT)	T[p]T-	−4.602	−4.548	−4.406	0.196	−0.420
		-TpT-	−4.094	−4.044	−3.903	0.191	+0.174
		-pT	−4.226	−4.166	−4.013	0.213	−0.021
A	d(T[p]TpT[p]T)	T[p]-	−4.586	−4.539	−4.393	0.193	−0.404
		-TpT-	−3.781	−3.758	−3.663	0.118	+0.487
		-[p]T	−4.548	−4.527	−4.452	0.095	−0.343

[a] Chemical shift values in ppm (±0.005) from internal TMP. [b] Cis-syn photodimers, represented as T[p]T, are formed by photosensitized UV irradiation in aqueous acetone at −1.5 °C with 310-nm light. [c] HPLC fractions collected, labeled as shown in Figure 2. [d] $\Delta\delta = \delta(63\ °C) - \delta(18\ °C)$. [e] $\Delta\Delta\delta$ = δ(in photodimer oligomer) − δ(in unmodified oligomer) at 18 °C, e.g., δ[d(T[p]T)] − δ[d(TpT)]; (−) means an upfield shift. [f] n/a, not applicable.

= 6.0 Hz similar to the H6 protons observed in d(T[p]T) confirms the presence of the cis-syn configuration in both trimers and the tetramer fraction. Although not shown, a similar AB system in proton spectra of tetramer fractions A, C, and D also indicates the isolation of additional tetramers containing a cis-syn photodimer.

A variety of positional isomers may be formed in the thymine trimer and tetramer as described earlier. Assignment of the cis-syn ring to a specific position (e.g., 3′ end, 5′ end, interior) is done through a comparison of the proton NMR patterns with those of *cis-syn*-d(T[p]T). Unequivocal assignment to either isomer is made by assuming that the spectral pattern of the T[p]- and -[p]T nucleotides in the dimer would be similar to those observed for the T[p]- fragment in DpT and DpTpT and the -[p]T nucleotide in TpD and TpTpD, respectively. The spectral patterns shown in Figure 3 identify trimer fraction A as DpT by the upfield shift of the T[p]-H5′,H5″ pair at 3.71 ppm which lacks phosphorus coupling. The assignment of trimer fraction B as TpD is made by the shift to 4.35 ppm of the -[p]T H3′ which also lacks a phosphorus interaction and overlaps the -[p]T H6 doublet. In addition to these specific criteria, many other similarities in NMR parameters are observed between the respective terminal photodimer nucleotides, corroborating these trimer assignments. The absence of upfield-shifted T[p]- H5′,H5″ protons near 3.71 ppm, the lack of a -[p]T H3′ at about 4.35 ppm, and the presence of two sets of saturated H6 and CH_3 protons at 4.30–4.34 and 1.50 ppm, respectively, as well as other characteristics observed in common with both TpD and DpT confirm the identification of tetramer fraction B (Figure 3, bottom) as TpDpT. The similarities of the proton parameters observed for the other tetramer ^{1}H spectra with those for *cis-syn*-d(T[p]T), TpD, and DpT (Figure 3) identify the positional assignment of the remaining cis-syn tetramer photodimers. The unequivocal assignment of the trimer and tetramer cis-syn photodimers is therefore made via the presence of the upfield-shifted phosphorus resonance and the chemical shift positions of select protons.

Spectral Assignments. The procedure of direct chemical shift comparison between the simple model d(T[p]T) and longer (or more complicated) oligomers has been utilized to make resonance assignments in thymine oligomers containing cis-syn photodimers. Table I lists the ^{31}P NMR chemical shift values of such photodimers. In the case of d(TpTpT), the formation of a cis-syn photodimer (1) shifts the internal phosphate (-[p]-) upfield to between −4.47 and −4.57 ppm as observed in d(T[p]T) and (2) displaces the adjacent phosphodiesters downfield. Subsequent comparison with the trimer positions enables ^{31}P resonance assignments in the tetramers. The positions of neighboring phosphates in TpDpT are nearly identical with the same values observed in TpD and DpT and also show a great deal of similarity with resonances assigned as the -TpD in TpTpD and DpT- in DpTpT (Table I). Next nearest neighbor phosphodiesters such as Tp- in TpTpD and -pT in DpTpT have chemical shift positions much like those of the unmodified tetramer. Interestingly, the double dimer d(T[p]TpT[p]T) has two upfield resonances representing T[p]T regions and a resonance shifted far downfield (ca. 0.487 ppm) which is assigned as the phosphate between the photodimers.

Proton resonance assignments in both trimer models were made by using a two-step procedure. Initially, select resonances were compared with resonance positions in *cis-syn*-d(T[p]T) (Figure 3; Table II) and assigned as described earlier. Then, 2-D COSY and high-field phosphorus-decoupled proton acquisitions were essential to complete a first-order analysis of all three trimer models due to resonance overlap. Assignment of H5′,H5″ protons were made in accordance with the procedure of Remin and Shugar (1972). ^{1}H NMR parameters for d(TpTpT) and both cis-syn photodimers were then refined iteratively by computer simulation (using PANIC[2]) and are listed in Table III. A similar two-step procedure facilitated resonance assignments for virtually all hydrogens in tetramer oligomers following trimer assignments. The tetramer photodimer possessing both adjacent nucleotides warranted more extensive proton NMR studies. The ^{1}H NMR parameters of *cis-syn*-TpDpT which are partially refined by computer simulation are compared with those of d(TpTpTpT) in Table IV. Some parameters are not determined as accurately as others due to resonance overlap and consequently are quoted to less

Table II: ^{1}H NMR Parameters[a] for d(TpT) and *cis-syn*-d(T[p]T)

parameter	d(TpT)[b]		*cis-syn*-d(T[p]T)		$\Delta\delta$[c]	
	dTp-	-pdT	dT[p]-	-[p]dT	dT[p]-	-[p]dT
$\delta_{H1'}$	6.2102	6.3164	5.6971	5.9930	−0.5131	−0.3234
$\delta_{H2'}$	2.3547	2.3869	2.6246	2.3085	0.2699	−0.0784
$\delta_{H2''}$	2.5677	2.3744	2.4064	2.1149	−0.1613	−0.2595
$\delta_{H3'}$	4.7866	4.6013	4.6635	4.3393	−0.1231	−0.2620
$\delta_{H4'}$	4.1923	4.1381	4.1500	3.9353	−0.0423	−0.2028
$\delta_{H5'}$	3.8410	4.1601	3.7361	4.1222	−0.1049	−0.0379
$\delta_{H5''}$	3.7947	4.0942	3.6976	4.0029	−0.0971	−0.0913
δ_{CH_3}	1.8778	1.8958	1.4921	1.5367	−0.3857	−0.3591
δ_{H6}	7.6703	7.6985	4.2690	4.3406	−3.4013	−3.3579
$^3J_{1'2'}$	7.49	6.83	8.59	8.69		
$^3J_{1'2''}$	6.14	6.86	5.40	5.77		
$^2J_{2'2''}$	−14.08	−14.14	−13.58	−13.65		
$^3J_{2'3'}$	6.49	7.00	5.42	7.85		
$^3J_{2''3'}$	3.43	3.83	3.26	3.42		
$^3J_{3'4'}$	3.42	3.83	3.02	4.81		
$^3J_{4'5'}$	3.42	2.62	3.97	1.67		
$^3J_{4'5''}$	4.50	3.30	3.93	6.73		
$^2J_{5'5''}$	−12.58	−11.52	−12.34	−11.85		
$^3J_{p3'}$	6.54		3.25			
$^4J_{p4'}$		2.41		1.51		
$^3J_{p5'}$		4.32		4.32		
$^3J_{p5''}$		4.23		5.59		
$^4J_{m6}$	1.25	1.25				
$^3J_{66}$			6.03	6.03		

[a] Chemical shift values (δ) in ppm (±0.002) from TSP; coupling constants (J) in Hz (±0.08). Data accumulated in D_2O at 30 °C and reported in Rycyna and Alderfer (1985). [b] Data accumulated in D_2O at 24 °C.

Table III: ^{1}H NMR Parameters[a] for d(TpTpT) and Cis-Syn Photodimers of d(TpTpT)

parameter	d(TpTpT)			*cis-syn*-d(TpT[p]T)			*cis-syn*-d(T[p]TpT)		
	Tp-	-pTp-	-pT	Tp-	-pT[p]-	-[p]T	T[p]-	-[p]Tp-	-pT
$\delta_{H1'}$	6.214	6.295	6.305	6.303	5.803	5.986	5.706	5.940	6.351
$\delta_{H2'}$	2.336	2.370	2.370	2.393	2.544	2.255	2.628	2.311	2.372
$\delta_{H2''}$	2.550	2.550	2.370	2.554	2.550	2.033	2.404	2.265	2.384
$\delta_{H3'}$	4.792	4.891	4.590	4.801	4.722	4.404	4.660	4.700	4.587
$\delta_{H4'}$	4.192	4.332	4.144	4.208	4.184	3.888	4.134	4.108	4.182
$\delta_{H5'}$	3.830	4.144	4.159	3.829	4.002	4.149	3.737	4.129	4.136
$\delta_{H5''}$	3.788	4.010	4.010	3.791	3.986	4.045	3.698	4.034	4.081
δ_{CH_3}	1.897	1.885	1.907	1.907	1.511	1.514	1.472	1.526	1.948
δ_{H6}	7.686	7.650	7.695	7.657	4.307	4.380	4.281	4.336	7.747
$^3J_{1'2'}$	7.65	8.08	6.89	7.91	9.17	9.17	8.46	9.61	7.56
$^3J_{1'2''}$	6.10	6.13	6.94	6.20	4.77	5.57	5.48	5.11	6.40
$^2J_{2'2''}$	−14.11	−14.15	*b*	−14.40	−13.61	−13.65	−13.71	−13.74	−14.10
$^3J_{2'3'}$	6.41	6.38	5.33	6.48	5.44	8.00	5.57	7.05	6.63
$^3J_{2''3'}$	3.18	3.09	5.38	3.11	2.19	3.13	3.58	2.53	3.38
$^3J_{3'4'}$	3.36	2.99	3.72	3.36	2.63	5.09	3.34	4.03	3.21
$^3J_{4'5'}$	3.42	2.57	2.69	3.45	3.61	1.61	3.72	1.70	2.80
$^3J_{4'5''}$	4.62	3.08	3.57	4.77	4.65	5.57	3.84	6.26	3.43
$^2J_{5'5''}$	−12.55	−11.73	−11.72	−12.54	−11.32	−12.17	−12.38	−11.76	−11.61
$^3J_{p3'}$	6.48	6.28		6.82	4.19		3.82	6.55	
$^4J_{p4'}$		2.64	2.49		1.36	1.85		1.58	2.47
$^3J_{p5'}$		4.50	4.53		5.08	4.65		4.25	4.95
$^3J_{p5''}$		4.40	4.68		4.80	4.23		5.15	4.95
$^4J_{m6}$	1.23	1.22	1.22	1.23					1.26
$^3J_{66}$					6.18	6.18	6.00	6.00	

[a] Chemical shift values (δ) in ppm (±0.0003) from TSP; coupling constants (J) in Hz (±0.15). Data accumulated in D_2O at 30 °C. [b] $J_{2'2''}$ is arbitrary when $\delta_i = \delta_j$.

significant digits. A comparison of the parameters of TpD and DpT with those of TpDpT shows a near juxtaposition of the TpT[p]- fragments in TpD with the -[p]TpT nucleotides in DpT; however, some anomolies are observed in the coupling constants.

Carbon-13 resonance positions were obtained in the oligothymidylates by two methods. First, resonances were initially assigned in the usual stepwise fashion beginning with the parameters for *cis-syn*-d(T[p]T) reported by Rycyna and Alderfer (1985). Next, positions of all protonated carbons were confirmed by the off-resonance proton-decoupling technique following the assignment of the proton spectra (Tables III and IV). Tentative assignments are made for carbonyl carbons. ^{13}C NMR parameters for d(TpTpT) are compared with those for *cis-syn*-TpD and -DpT in Table V; Table VI lists the ^{13}C NMR parameters for d(TpTpTpT) and *cis-syn*-TpDpT. As observed in the proton parameters, the carbon spectral characteristics of TpDpT are similar to those possessed by the analogous nucleotides in *cis-syn*-TpD and -DpT. All furanose carbons in TpDpT are assigned on the basis of expected positions from TpD and DpT as well as the off-resonance proton-decoupling technique. C2 and C4 carbons are assigned to either a saturated or unsaturated nucleotide while C5, C6, and CH_3 were labeled according to positions in the trimers. The carbons in unmodified d(TpTpTpT) were designated to a carbon type; however, unambiguous assignment

Table IV: ^{1}H NMR Parameters[a] for d(TpTpTpT) and *cis-syn*-d(TpT[p]TpT) Photodimer

	d(TpTpTpT)[b]				*cis-syn*-d(TpT[p]TpT)			
parameter	Tp-	-pTp-	-pTp-	-pT	Tp-	-pT[p]-	-[p]Tp-	-pT
$\delta_{H1'}$	6.219	6.284	6.291	6.293	6.309	5.809	5.963	6.352
$\delta_{H2'}$	2.34	2.38	2.38	2.38	2.387	2.538	2.269	2.367
$\delta_{H2''}$	2.57	2.57	2.57	2.38	2.540	2.539	2.181	2.367
$\delta_{H3'}$	4.283	4.92	4.90	4.589	4.83	4.76	4.71	4.589
$\delta_{H4'}$	4.199	4.35	4.35	*c*	4.212	4.186	4.06	4.18
$\delta_{H5'}$	3.856	4.15	4.15	4.15	3.821	3.999	4.16	4.132
$\delta_{H5''}$	3.804	4.14	4.14	4.14	3.788	3.990	4.07	4.086
δ_{CH_3}	1.892	1.892	1.880	1.901	1.904	1.498	1.504	1.941
δ_{H6}	7.685	7.666	7.646	7.696	7.671	4.301	4.399	7.755
$^3J_{1'2'}$	7.5	8.2	8.0	6.9	7.97	8.94	9.62	7.01
$^3J_{1'2''}$	6.2	5.5	5.5	6.9	6.05	5.36	5.22	7.01
$^2J_{2'2''}$	−14.0	−14.0	−14.0	*c*	−14.30	−13.61	−13.40	*c*
$^3J_{2'3'}$	6.5	5.2	5.2	5.2	6.60	4.3	7.69	4.94
$^3J_{2''3'}$	3.4	3.4	3.4	4.5	3.02	3.5	2.13	4.94
$^3J_{3'4'}$	3.5	2.9	2.9	3.4	2.75	*c*	*c*	2.75
$^3J_{4'5'}$	3.7	*c*	*c*	*c*	3.57	3.57	*c*	2.71
$^3J_{4'5''}$	4.5	*c*	*c*	*c*	4.67	4.71	*c*	3.14
$^2J_{5'5''}$	−12.5	*c*	*c*	*c*	−12.51	−11.3	−11.1	−11.75
$^3J_{p3'}$	6.5	6.4	6.4		6.87	*c*	6.52	
$^4J_{p4'}$		*c*	*c*	*c*		1.4	*c*	2.31
$^3J_{p5'}$		*c*	*c*	*c*		4.89	4.50	4.77
$^3J_{p5''}$		*c*	*c*	*c*		4.71	*c*	4.57
$^4J_{m6}$	1.23	1.24	1.22	1.23	1.25			1.26
$^3J_{66}$						6.12	6.12	

[a] Chemical shift values (δ) in ppm (±0.01) from TSP; coupling constants (J) in Hz (±0.3). Data were approximated only by first-order analysis and have not undergone computer simulation. Parameters reported to less significant digits have larger standard deviation. Data accumulated at 30 °C. [b] Resonances not assigned unambiguously. [c] Unable to be determined due to resonance overlap and/or pattern complexity.

Table V: ^{13}C NMR Parameters[a] for d(TpTpT) and Cis-Syn Photodimers of d(TpTpT)

	d(TpTpT)[b]			*cis-syn*-d(TpT[p]T)			*cis-syn*-d(T[p]TpT)		
parameter	Tp-	-pTp-	-pT	Tp-	-pT[p]-	-[p]T	T[p]-	-[p]Tp-	-pT
$\delta_{C1'}$	18.58	18.26	18.34	18.55	19.73	18.95	20.59	18.90	18.54
$\delta_{C2'}$	−28.90	−29.05	−27.79	−28.99	−33.06	−30.49	−33.02	−31.17	−27.77
$\delta_{C3'}$	8.84	8.58	4.03	8.56	8.46	1.80	8.84	6.51	4.31
$\delta_{C4'}$	19.13	17.50	18.55	19.09	15.38	16.62	16.39	15.78	18.74
$\delta_{C5'}$	−5.45	−1.68	−1.64	−5.44	−1.82	−1.62	−5.45	−1.46	−1.46
δ_{C2}[c]	85.66	85.56	85.56	85.11	87.13	87.62	87.11	87.60	85.14
δ_{C4}[c]	100.68	100.37	100.50	99.98	106.53	105.90	106.63	105.85	99.91
δ_{C5}[c]	44.96	44.96	45.11	45.00	−17.31	−17.58	−15.66	−19.90	45.04
δ_{C6}[c]	70.77	70.57	70.70	71.02	−8.30	−10.49	−6.98	−10.90	70.86
δ_{CH_3}	−54.90	−54.90	−54.83	−55.11	−49.93	−49.41	−49.70	−49.70	−54.91
$^3J_{pC2'}$	3.1	3.0		3.4	<0.5		3.6	3.3	
$^2J_{pC3'}$	5.0	5.3		5.4	5.5		5.7	5.1	
$^3J_{p3'C4'}$	7.4	8.2		6.4	9.4		7.7	7.9	
$^3J_{p5'C4'}$		8.2	9.0		9.4	8.6		7.9	8.5
$^2J_{pC5'}$		5.8	5.6		5.9	5.2		5.2	5.2

[a] Chemical shift values (δ) in ppm (±0.003) from dioxane; coupling constants (J) in Hz (±0.27). Data accumulated in D_2O at 30 °C. [b] Base carbon resonances not assigned unambiguously. [c] Saturated carbon resonances in photodimers not assigned unambiguously.

Table VI: ^{13}C NMR Parameters[a] for d(TpTpTpT) and *cis-syn*-d(TpT[p]TpT) Photodimer

	d(TpTpTpT)[b]				*cis-syn*-d(TpT[p]TpT)			
parameter	Tp-	-pTp-	-pTp-	-pT	Tp-	-pT[p]-	-[p]Tp-	-pT
$\delta_{C1'}$	18.60	18.31	18.31	18.35	18.47	19.47	18.96	18.47
$\delta_{C2'}$	−28.92	−28.98	−28.98	−27.82	−29.03	−33.05	−31.38	−27.72
$\delta_{C3'}$	9.27	8.89	8.53	4.05	8.56	8.41	5.95	4.37
$\delta_{C4'}$	19.14	17.69	17.52	18.58	19.03	15.25	15.64	18.72
$\delta_{C5'}$	−5.46	−1.47	−1.54	−1.60	−5.37	−2.21	−1.61	−1.50
δ_{C2}[c]	85.09	84.92	84.92	84.92	85.04	87.52	87.03	85.00
δ_{C4}[c]	99.82	99.58	99.58	99.72	99.86	106.42	105.60	99.80
δ_{C5}[c]	44.86	44.92	45.02	45.05	44.93	−17.40	−17.48	44.88
δ_{C6}[c]	70.81	70.67	70.59	70.78	70.87	−8.55	−10.34	70.69
δ_{CH3}[d]	−55.02	−55.02	−54.99	−54.94	−55.05	−49.87	−49.37	−54.85
$^3J_{pC2'}$	4.4	4.1	4.1		4.1	2.2	3.8	
$^2J_{pC3'}$	5.3	5.3	5.4		5.6	5.3	5.6	
$^3J_{p3'C4'}$	7.2	7.5	7.5		6.3	8.9	6.8	
$^3J_{p5'C4'}$		9.0	8.4	8.7		8.9	7.7	8.5
$^2J_{pC5'}$		6.1	*e*	6.4		6.2	5.0	5.4

[a] Chemical shift values (δ) in ppm (±0.003) from dioxane; coupling constants (J) in Hz (±0.272). Data accumulated in D_2O at 30 °C. [b] Base and phosphorus-coupled resonances not assigned unambiguously. [c] Base resonances within saturated or unsaturated nucleotides of d(TpT[p]TpT) are not assigned unambiguously. [d] Resonances on unsaturated bases of d(TpT[p]TpT) not assigned unambiguously. [e] Unable to be determined due to resonance overlap.

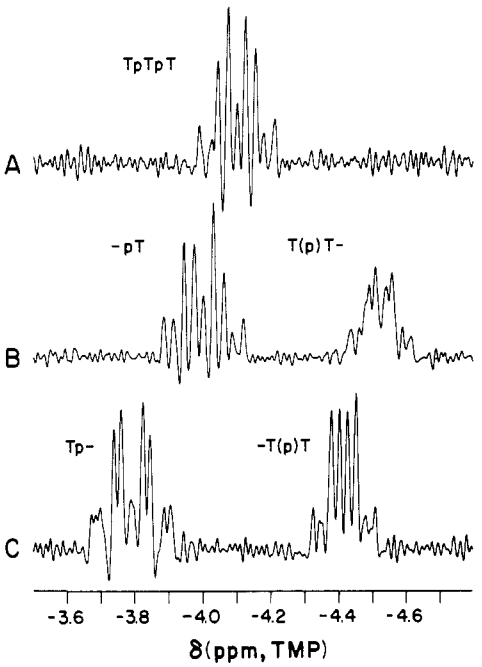

FIGURE 4: Phosphorus-31 (proton-coupled) NMR spectra at 30 °C of (A) d(TpTpT), (B) *cis-syn*-d(T[p]TpT), and (C) *cis-syn*-d(TpT-[p]T).

to a specific nucleotide is only possible for C2′, C3′, and C5′ carbons lacking a phosphorus interaction and for terminal C1′ and C4′ carbons.

Cis-Syn Photodimerization Effects. An abundance of multinuclear NMR data (Tables I–VI) show corroborative effects of forming a cis-syn T[p]T photodimer on the NMR parameters of thymine oligomers. In general, the chemical shift positions of phosphodiesters between cis-syn cyclobutyl-linked thymines are shifted far upfield ($\Delta\Delta\delta$ = −0.375 ± 0.07 ppm) and have a small dependence on temperature ($\Delta\delta$ = 0.144 ± 0.057 ppm) relative to unmodified thymine nucleotides. By contrast, the chemical shift positions of both phosphodiesters adjacent to the dimer are shifted downfield. The phosphodiester on the 3′ side (e.g., -pT) moves only slightly downfield ($\Delta\Delta\delta$ = +0.092 ± 0.082 ppm) while the one on the 5′ side (Tp-) is displaced much farther ($\Delta\Delta\delta$ = 0.313 ± 0.007 ppm). Interestingly, the Tp- resonance is not as temperature dependent ($\Delta\delta$ = 0.148 ± 0.006 ppm) as the -pT resonance ($\Delta\delta$ = 0.223 ± 0.023 ppm). Qualitative effects of photodimerization on the phosphodiester regions of the adjacent nucleotides in TpD and DpT are obtained from proton-coupled ^{31}P NMR data (Figure 4). Dissimilar patterns are observed for the neighboring phosphodiesters at −4.06 and −3.85 ppm. The resemblance in patterns between unmodified d(TpTpT) and the -pT in DpT is not unexpected considering their similar chemical shift positions and $\Delta\delta$ values (Table I). The proton-coupled ^{31}P NMR data (not shown) of d(TpTpTpT) and the four positional cis-syn isomers also illustrate a variety of patterns; the nucleotides adjacent to the -T[p]T- in TpDpT display patterns similar to those of the Tp- and -pT phosphodiesters in TpD and DpT. Therefore, although the ^{31}P NMR data are simple in appearance, the effects of cis-syn photodimerization on the phosphorus spectral characteristics are dramatic and conspicuous.

The proton NMR parameters for cis-syn oligothymidylates show several general changes due to photodimerization. All chemical shift values reported at 18 and 63 °C in *cis-syn*-d(T[p]T) shift upfield relative to unmodified d(TpT) except for the T[p]- H2′, which is shifted downfield 0.27 ppm (Hruska et al., 1975). A similar observation is made at 30 °C for *cis-syn*-d(T[p]T) (Table II) and the cis-syn trimers (Table III) and tetramers (Table IV) examined here. The largest changes occur in the heterocyclic base (H6 and CH_3) due to ring saturation as observed by Kan et al. (1982) and in the deoxyfuranose hydrogens proximal to the base. Conformational alterations in the furanose moieties of the photodimer are indicated by large changes in the $J_{H,H}$ and $J_{H,P}$ values consistent with the parameters reported by Hruska et al. (1975). In the manner that the proton-coupled ^{31}P data show different patterns in the phosphodiester regions adjacent to the photodimer (Figure 3), changes in these regions are indicated quantitatively in exocyclic coupling constants listed in Tables III and IV. Specifically, the $J_{H3',P}$ in Tp- and the $J_{4'5'}$, $J_{4'5''}$, $J_{H4',P}$, $J_{H5',P}$, and $J_{H5'',P}$ in the -pT[p]- nucleotides of TpD and TpDpT undergo major rearrangements. Kemmink et al. (1987) have also reported changes in the positions of many protons in d(GCGTTGCG)·d(CGCAACGC) due to the formation of a cis-syn -T[p]T- photodimer. Alterations in the furanose chemical shift positions observed in the oligothymidylates (Tables II–IV) were compared with analogous protons in the -GpT[p]TpG- nucleotides (Kemmink et al., 1987). Similarities are observed in the magnitudes and directions of modulations of many chemical shift positions in both studies; however, two differences are noted. First, photodimerization in the oligothymidylates induces a greater upfield shift in the -T[p]- H1′ (0.48–0.51 ppm) than in the -[p]T- H1′ (0.33 ppm) whereas Kemmink et al. (1987) report a larger upfield shift for the T5 (or -[p]T-) H1′ (0.54 ppm) than for the T4 (or -T[p]-) H1′ (0.42 ppm). Furthermore, an abundance of spin-simulated ^{1}H NMR parameters (Tables II–IV) indicates the -T[p]- H1′ resonates upfield (av 5.75 ppm) of the -[p]T- H1′ (av 5.97 ppm); on the other hand, Kemmink et al. (1987) report that the T4 (or -T[p]-) H1′ resonates downfield (5.60 ppm) from the T5 (or -[p]T-) H1′ at 5.39 ppm. It is interesting to mention that the difference between the -T[p]- and -[p]T- chemical shift positions in both studies is virtually identical (0.21–0.22 ppm). Since 2-D COSY scalar correlations (not shown) were traced from the H1′s to the remaining deoxyfuranose protons known to possess or lack a phosphorus interaction, it is unlikely that incorrect H1′ assignments were made in the oligothymidylates. The other difference noted between these data is the effect on the -T[p]-H2′,H2″ pair due to photodimerization. Kemmink et al. (1987) report the T4 (or -T[p]-) H2′ and H2″ move upfield 0.16 and 0.04 ppm, respectively, while the data in Tables II–IV show the -T[p]- H2′ shifts downfield 0.22 ppm and the H2″ moves upfield 0.09 ppm.

Finally, ^{13}C NMR data of the thymine oligomers (Tables V and VI) show a variety of changes upon induction of a cis-syn photodimer. The largest effects are upfield shifts of C5, C6, and CH_3 belonging to the saturated bases. Except for C5′, all of the sugar carbons are affected in varying degrees, usually as an upfield shift, thus corroborating with the proton data (Tables II–IV). Important changes are also observed in the $J_{C,P}$ values upon photodimer formation. For example, the Tp- $J_{pC2'}$ increases from 3.1 Hz in d(TpTpT) to 3.4 Hz in TpD, and the $J_{p3'C4'}$ decreases from 7.4 to 6.4 Hz. Alterations in the ^{31}P chemical shift positions in conjunction with the proton–proton, proton–phosphorus, and carbon–phosphorus coupling constants have conformational implications regarding the exocyclic region on the 5′ side of the photodimer.

Discussion

The influence of a cis-syn photodimer on the conformation of adjacent thymine nucleotides was investigated by using NMR spectroscopy in UV-irradiated d(TpTpT) and d-

Table VII: Calculated Furanose Conformations of Oligothymidylates Containing Cis-Syn Photodimers

		furanose distribution[a]							
		form I			form II				
oligomer	nucleotide	f_I	P_I	C_I	f_{II}	P_{II}	C_{II}	Φ	error (Hz)[b]
d(TpT)	dTp-	0.29	−10.7	${}_2^3T$	0.71	151.6	${}^2T_1$	35	0.43
	-pT	0.35	1.0	${}_2^3T$	0.65	155.3	${}^2T_1$	31	0.33
d(TpTpT)	dTp-	0.26	−7.3	${}_2^3T$	0.74	153.1	${}^2T_1$	34	0.80
	-pTp-	0.23	−7.2	${}_2^3T$	0.77	155.4	${}^2T_1$	34	0.24
	-pT	0.39	21.6	${}^3E$	0.61	183.6	${}_3^2T$	42	0.85
d(TpTpTpT)	dTp-	0.28	−5.7	${}_2^3T$	0.72	152.4	${}^2T_1$	34	0.60
	-pTp-	0.23	0.0	${}_2^3T$	0.77	160.3	${}^2E$	41	0.48
	-pTp-	0.25	−7.2	${}_2^3T$	0.75	162.5	${}^2E$	40	0.82
	-pT	0.33	11.0	${}^3T_2$	0.67	190.0	${}_3T^2$	41	0.30
d(T[p]T)	dT[p]-	0.21	5.9	${}^3T_2$	0.79	153.5	${}^2T_1$	41	0.21
	-[p]T	0.19	−11.8	${}_2^3T$	0.81	120.4	${}_1T^0$	37	0.91
d(TpT[p]T)	dTp-	0.24	−0.4	${}^3T_2$	0.76	151.7	${}^2T_1$	34	0.49
	-pT[p]	0.13	−15.0	${}_2E$	0.88	147.2	${}_1^2T$	42	0.94
	-[p]T	0.15	−25.0	${}_2^1T$	0.85	114.4	${}_1T^0$	42	0.70
d(T[p]TpT)	dT[p]-	0.24	9.1	${}^3T_2$	0.76	151.1	${}^2T_1$	41	0.13
	-[p]Tp-	0.12	−14.7	${}_2E$	0.88	126.8	${}_1E$	42	0.48
	-pT	0.27	−8.7	${}_2^3T$	0.73	156.0	${}^2T_1$	33	0.17
d(TpT[p]TpT)	dTp-	0.23	−21.9	${}_2E$	0.77	155.4	${}^2T_1$	33	0.36
	-pT[p]	0.21	28.5	${}^3T_4$	0.79	164.4	${}^2E$	46	0.75
	-[p]Tp-	0.09	−35.2	${}_2^1T$	0.91	121.2	${}_1T^0$	41	0.22
	-pT	c							

[a] Calculations are performed by using the program PSEUROT. The data are analyzed by assuming a two-state equilibrium (consisting of mole fractions f_I and f_{II}), with an amplitude of pucker Φ and phase angles P_I and P_{II} (deg); C_I and C_{II} are the corresponding envelope or twist notation that classify the sugar puckering modes (Altona & Sundaralingam, 1973). [b] This is the sum of the differences (absolute value) between the five experimental furanose coupling constants and their calculated values determined from f_I, f_{II}, P_I, P_{II}, and Φ. [c] Not calculated because $J_{1',2'}$, $J_{1',2''}$, $J_{2',3'}$, and $J_{2'',3'}$ are not uniquely determined since $\delta_{H2'} = \delta_{H2''}$.

(TpTpTpT). Prior to the analyses of these longer oligothymidylates, a complete understanding was established of the conformational properties of the entity responsible for inducing intrastrand distortion, the dinucleoside monophosphate photodimer. A previous 270-MHz proton NMR study (Hruska et al., 1975) revealed various conformational changes in d(TpT) upon formation of the cis-syn photodimer, d(T[p]T). The production of this same photodimer under different conditions and identification have also been reported with ^{1}H, ^{13}C, and ^{31}P NMR (Rycyna & Alderfer, 1985). Proton NMR parameters for *cis-syn*-d(T[p]T) listed in Table II are quite similar to those reported by Hruska et al. (1975). Minor deviations are observed because (1) the spectra were recorded at different temperatures and (2) our data were acquired at 200, 400, 500, and 600 MHz enabling better parameter refinement. The subsequent analysis of this multinuclear NMR data (Rycyna & Alderfer, 1985) provides a more complete understanding of d(T[p]T).

The development of a conformational picture for the cis-syn photodimer in solution requires an integration of the previous ^{1}H NMR study (Hruska et al., 1975) and the X-ray study (Cadet et al., 1985) with the current NMR (Rycyna & Alderfer, 1985) and molecular mechanics data (G. Raghunathan, T. Kieber-Emmons, R. Rein, and J. L. Alderfer, submitted for publication). Three aspects of the photodimer conformation are of importance. First, the furanose–base torsion angles in *cis-syn*-d(T[p]T) cyanoethyl ester have been reported by Cadet et al. (1985) to undergo interesting changes; namely, the dT[p]- χ(C1′–N1′) rearranges from the anti to the syn conformer while the -[p]dT fragment χ(C1′–N1) remains in the anti domain. The ^{1}H NMR (Table II) and ^{13}C NMR data (Rycyna & Alderfer, 1985) support this observation of different glycosyl conformations. In the dT[p]- fragment, the large $\Delta\delta$ values for H1′ (−0.51 ppm) and H2′ (+0.27 ppm) are consistent with a change in torsion angle χ(C1′–N1) (Giessner-Prette & Pullman, 1977) from the anti to syn domain (Hruska et al., 1985). The study of Schweizer et al. (1973) using C6-substituted pyrimidines which are not conformationally stable in the anti conformer shows upfield shifts for the C2′ carbon. Similar upfield shifts for C2′ are also observed for various purine-substituted bases in the syn range (Uesugi & Ikehara, 1977; Alderfer et al., 1984). The downfield shift of the dT[p]- C1′ (+2.32 ppm) and upfield shift of the dT[p]- C2′ (−4.01 ppm) support the change in glycosyl angles. Additional evidence of sugar–base torsion angle change comes from proton–carbon coupling constants. In d(TpT), both nucleotides have anti-type glycosyl bonds characterized by different coupling constant values, namely, $J_{C2,H1'}$ = 2.1 Hz and $J_{C2,H6}$ = 7.9–8.4 Hz. The C2 coupling constants in the photodimer are 4.17 and 4.29 Hz in dT[p]- and 1.66 and 5.48 Hz in -[p]dT. These values provide further evidence that the dT[p]- fragment has undergone a change consistent with an anti to syn conversion, whereas the -[p]dT portion remains essentially the same as in d(TpT).

An analysis of refined proton coupling constant data provides information about furanose conformations in d(T[p]T). The previous proton NMR study (Hruska et al., 1975) showed that the C2′-endo/C3′-endo furanose distribution in the dTp- to dT[p]- conversion was not markedly altered except for a slight shift to a higher C2′-endo percentage. They did however report a sizeable increase in the C3′-endo pucker for the -[p]dT furanose. In our study the experimental refined (computer-simulated) furanose coupling constants (Table IV) are used as the input data for analysis by PSEUROT.[3] The calculated furanose distributions, mole fractions, and errors between observed and calculated coupling constants are listed in Table VII. These results show virtually no change in the dT[p]- fragment as reported by Hruska et al. (1975). On the other hand, our analysis of -[p]dT indicates a predominant C1′-exo-type conformation (81%) with a minor contribution from the C2′-exo-type pucker (19%), which differs from the results

[3] PSEUROT: Computer-Assisted Pseudorotational Analysis of Five-Membered Rings by Means of Vicinal Proton Spin–Spin Coupling Constants; Quantum Chemistry Program Exchange, Program No. 463, Indiana University.

Table VIII: Rotamer Distributions of Exocyclic Bonds for Oligothymidylates

	γ(C5′–C4′)[a]			β(O5′–C5′)[b]			ϵ(C3′–O3′)[c]	
	g^+	t	g^-	t	g^+	g^-	g^-	t
d(TpT)								
dTp-	0.63	0.23	0.14				0.22	0.80
-pdT	0.74	0.21	0.05	0.84 (0.81)[d]	0.08	0.08		
cis-syn-d(T[p]T)								
dT[p]-	0.63	0.19	0.18				0.29	0.82
-[p]dT	0.51	0.49	0.00	0.74 (0.69)[d]	0.18	0.08		
d(TpTpT)								
dTp-	0.59	0.27	0.14				0.23	0.80
-pdTp-	0.83	0.11	0.05	0.80 (0.73)[d]	0.10	0.10	0.22	0.89
-pdT	0.77	0.16	0.07	0.78 (0.81)[d]	0.11	0.11		
cis-syn-d(TpT[p]T)								
dTp-	0.57	0.28	0.15				0.26	0.70
-pdT[p]-	0.57	0.27	0.16	0.75 (0.84)[d]	0.12	0.13	0.00	1.02
-[p]dT	0.68	0.36	0.00	0.80 (0.77)[d]	0.09	0.11		
cis-syn-d(T[p]TpT)								
dT[p]-	0.64	0.19	0.17				0.28	0.84
-[p]dTp-	0.59	0.43	0.00	0.78 (0.70)[d]	0.14	0.09	0.25	0.86
-pdT	0.78	0.14	0.08	0.75 (0.76)[d]	0.13	0.13		
cis-syn-d(TpT[p]TpT)								
dTp-	0.57	0.27	0.16				0.13	0.69
-pdT[p]-	*e*	*e*	*e*	0.77 (0.80)[d]	0.11	0.12	0.34	0.97
-[p]dTp-	0.57	0.28	0.16	*e* (0.68)[d]	*e*	0.10	0.30	0.74
-pdT	0.81	0.11	0.07	0.78 (0.76)[d]	0.11	0.12		

[a] Karplus equation ($J_{H,H} = 10.5 \cos^2 \phi - 1.2 \cos \phi$) from Altona and Sundaralingam (1973) and rotamer equations from Davies and Danyluk (1974). [b] Karplus equation ($J_{H,P} = 15.3 \cos^2 \phi - 6.1 \cos \phi + 1.6$) from Lankhorst et al. (1984) and rotamer equations from Davies and Danyluk (1974). [c] Equations used: $f_{g^-} = (J_{pC2'} - 1.0)/9.2$; $f_t = J_{p3'C4'}/9.2$ (Alderfer & Ts'o, 1977). Equations from Davies and Danyluk (1974) have been slightly modified because we observed that $J_{pC2'} + J_{p3'C4'}$ in many ribo dimers is 9.2 ± 0.2 Hz and in deoxy dimers is 10.2 ± 0.2 Hz. Accordingly, $J_{pC2'}$ is reduced 1.0 Hz. [d] Equation used: $f_t = (J_{p5'C4'} - 0.73)/10.27$; $J_{C,P} = 6.9 \cos^2 \phi + 0.7$ (Lankhorst et al., 1984). [e] Unable to determine due to lack of necessary coupling constants.

of Hruska et al. (1975). Our molecular mechanics study reveals low-energy forms of C4′-exo and O4′-endo/C1′-exo for -[p]dT, while the conformation obtained in the X-ray study of this furanose is $^3T_4$ (Cadet et al., 1985). Collectively, these data indicate a similar trend of conformational change occurs for the -[p]dT portion of the molecule, toward a lower pseudorotational phase angle.

Conformational properties of three exocyclic bonds (shown in Figure 5) in the photodimer were calculated from $J_{H,H}$, $J_{H,P}$, and $J_{C,P}$ values [Table II and Rycyna and Alderfer (1985)] and are represented as rotamer distributions (Table VIII). The population of bonds γ(C5′–C4′) and β(O5′–C5′) are obtained by using a three-state model and that of bond ϵ-(C3′–O3′) by using a two-state model (Alderfer & Ts'o, 1977). These distributions are qualitatively similar to those reported by Hruska et al. (1975) although differences in coupling constants and Karplus-type equations used to determine the populations result in slightly different values. A comparison of the populations between d(T[p]T) and d(TpT) reveal the effects of photodimer formation. The rotamer populations of γ(C5′–C4′) in dT[p]- are unaltered from the unmodified dimer. In contrast, the gauche$^+$ rotamer of this bond in -[p]dT is markedly reduced, from 74% to 51%. The populations of the trans rotamer of β(O5′–C5′) in d(TpT) were obtained independently from ^{1}H and ^{13}C data and were found to agree quite well. Upon photodimerization, the trans rotamer of β(O5′–C5′) is depopulated by about 10%. In the event the H5′ and H5″ protons are assigned incorrectly, the effect is to interchange the gauche$^-$ with the trans rotamers in γ-(C5′–C4′) and the gauche$^+$ with the gauche$^-$ rotamers in β(O5′–C5′). Table VIII shows that the interchange would have no effect on the population of the major rotamer [e.g., gauche$^+$ in γ(C5′–C4′) and trans in β(O5′–C5′)] for either exocyclic bond; however, the change would alter the interpretation of the minor distributions for -[p]dT γ(C5′–C4′). In the case of ϵ(C3′–O3′), a small increase is observed in the gauche$^-$ rotamer, thus generating an inconsistency in the g$^-$,t

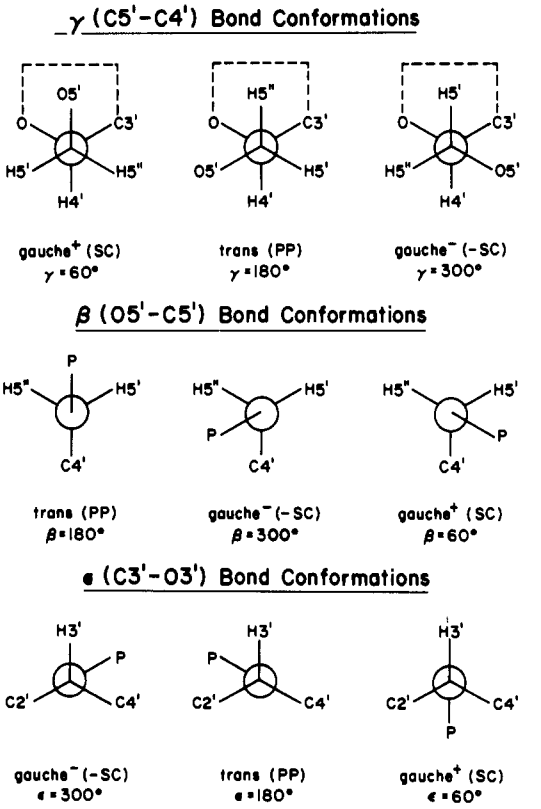

FIGURE 5: Structural representation of the dihedral angles for three nucleic acid exocyclic bonds, γ(C5′–C4′), β(O5′–C5′), and ϵ(C3′–O3′).

distribution. The fractional sum (1.11 rather than 1.0) is a result of the larger $J_{pC2'}$ and $J_{p3'C4'}$ (11.2 Hz); normally this sum is 10.2 ± 0.2 Hz for deoxy dimers (Alderfer, unpublished results). Consequently, the freely interconverting rotamer model may not best describe the conformational properties of ϵ(C3′–O3′) and perhaps other exocyclic bonds in *cis-syn*-d-(T[p]T) because of the high potential for restricted rotation

Table IX: Rigid-Angle Analysis of Exocyclic Bonds in Cis-Syn Oligothymidylates

J	Hz	Karplus angles (deg)	dihedral angles (deg)	J	Hz	Karplus angles (deg)	dihedral angles (deg)
			cis-syn-d(T[p]T)				
		dT[p]- γ(C5′–C4′)[a]				-[p]dT γ(C5′–C4′)	
$J_{4'5'}$	3.97	±47	73, 167	$J_{4'5'}$	1.67	±62	58, 182
		±124	356, 244			±110	10, 230
$J_{4'5''}$	3.93	±47	47, 313	$J_{4'5''}$	6.73	±30	30, 330
		±123	123, 237			±138	138, 222
best combination			240 ± 3				226 ± 4
		dT[p]- ϵ(C3′–O3′)[b]				-[p]dT β(O5′–C5′)	
$J_{pC2'}$	3.7	±18	138, 102	$J_{p5'}$	4.32	±48	72, 168
		±117	237, 3			±105	225, 15
$J_{p3'C4'}$	7.5	±140	220, 140	$J_{p5''}$	5.59	±41	199, 281
$J_{p3'}$	3.25	±54	186, 294			±110	130, 350
		±100	140, 340	$J_{p5'C4'}$	7.8	±142	218, 142
best combination			214 ± 21				214 ± 11
			cis-syn-d(TpT[p]T)				
		dTp- ϵ(C3′–O3′)[b]				-pT[p]- γ(C5′–C4′)	
$J_{pC2'}$	3.4	±23	143, 97	$J_{4'5'}$	3.61	±49	169, 71
		±115	235, 5			±122	242, 358
$J_{p3'C4'}$	6.4	±134	134, 226	$J_{4'5''}$	4.65	±43	43, 317
$J_{p3'}$	6.82	±35	275, 205			±127	127, 233
		±114	354, 126				
best combination			222 ± 12				237 ± 4

[a] Karplus-type equation from Altona and Sundaralingam (1973): $J_{H,H} = 10.5 \cos^2 \phi - 1.2 \cos \phi$. [b] Karplus-type equations used from Lankhorst et al. (1984): $J_{H,P} = 15.3 \cos^2 \phi - 6.1 \cos \phi + 1.6$; $J_{C,P} = 6.9 \cos^2 \phi - 3.4 \cos \phi + 0.7$.

due to the cyclobutane ring. Recently, a similar situation has been reported for a d(TpT) photoadduct (Rycyna & Alderfer, 1985).

An alternate interpretation of the conformations of exocyclic bonds can be made in terms of rigid angles. The $J_{H,H}$, $J_{H,P}$, and $J_{C,P}$ values were used to determine fixed conformational parameters by using Karplus-type relationships; the calculated dihedral angles for *cis-syn*-d(T[p]T) are listed in Table IX. Optimal approximation of the ϵ(C3′–O3′) dihedral angle requires three values. The $J_{pC2'}$ (3.7 Hz), $J_{p3'C4'}$ (7.5 Hz), and $J_{pH3'}$ (3.25 Hz) translate into ϕ(C2′,P) = ±18° (or ±117°), ϕ(C4′,P) = ±140°, and ϕ(H3′,P) = ±35° (or ±114°), respectively. A combination of torsion angles yield dihedral angles that could fall into one of two groups: 138–140° or 186–237°. The former group is energetically unfavorable, leaving the latter (average = 214 ± 21°) the most likely combination. In the X-ray study of d(T[p]T), this bond has a value of 207.1° while the molecular mechanics study (G. Raghunathan, T. Kieber-Emmons, R. Rein, and J. L. Alderfer, submitted for publication) reveals four minimum-energy conformations within the range 184–198°. Therefore, the crystallographic value, the NMR-determined rigid angle, and minimum-energy value for ϵ(C3′–O3′) fall in the range 198–214°. Such results encouraged rigid-angle calculations of two other exocyclic bonds in *cis-syn*-d(T[p]T), -[p]dT β-(O5′–C5′) and γ(C5′–C4′). Evaluation of β(O5′–C5′) also requires three coupling constants: $J_{p5'}$, $J_{p5''}$, and $J_{p3'C4'}$. One NMR solution (214 ± 11°) is reasonably close to the X-ray value (235°) and near a molecular mechanics derived value (214°; calculated range: 204–237°). The -[p]dT γ(C5′–C4′) is calculated from $J_{4'5'}$ and $J_{4'5''}$; neither of the NMR values is especially close to the X-ray value (189°) but in the range (208–275°) of the molecular mechanics values. Finally, although dT[p]- γ(C5′–C4′) is expected to rotate rapidly on the NMR time scale and exhibits a typical gauche$^+$ rotamer value (0.63; Table VIII), the rigid-angle value (240°) is energetically prohibited due to an eclipsed conformation. Nevertheless, this value provides the best agreement with the X-ray value (295.5°).

The quantitative changes in the ^{31}P resonance position for d(T[p]T) as a function of temperature (Table I) may be explained by the partially rigid nature of the exocyclic bonds as discussed above. On the one hand, the ^{31}P chemical shift value of a rigid nucleotide such as 3′,5′-cUMP is temperature independent between 18 and 63 °C (unpublished results) and is attributed to constrained phosphodiester angles (Gorenstein, 1978). On the other hand, polynucleotides show a strong temperature dependency in the same temperature range, a result of additional conformational degrees of freedom in the phosphodiester region. The small temperature-dependent chemical shift value of d(T[p]T) relative to that of d(TpT) (Table I) is consistent with a reduction in the ability of the furanose–phosphate backbone to undergo the normal range of correlated motions due to the constraints of the cyclobutane ring.

In establishing a better understanding of the conformation of d(T[p]T) in solution, multinuclear spectral patterns have been identified and characterized, thereby enabling the study of longer oligothymidylates containing cis-syn photodimers. Photosensitized UV irradiation of d(TpTpT) forms predominantly two positional cis-syn photodimers, TpD and DpT. A comparison of the data in Tables I–III and Table V indicates the cis-syn photodimer nucleotides in d(T[p]T) and both TpD and DpT have nearly identical NMR parameters. These resemblances are expected because of the constrained conformational nature of the cis-syn isomer and imply conformational homology in the photodimers. For instance, the cyclobutane ring conformations must be nearly the same because the J_{66} value (6.03 Hz) in d(T[p]T) lies in the range observed for TpD and DpT (6.00–6.18 Hz). Also, only modest differences are observed for the furanose conformations (Table VII) in the dT[p]- fragments of d(T[p]T) and d(T[p]TpT) as well as the -[p]dT nucleotides of d(T[p]T) and d(TpT[p]T): (1) the dT[p]- nucleotide in d(T[p]T) is 79% C2′-endo type ↔ 21% C3′-endo type while the -pT[p]- in d(TpT[p]T) is 88% C2′-endo type ↔ 13% C2′-exo, and (2) the -[p]dT in d(T[p]T) is 81% C1′-exo type ↔ 19% C2′-exo type, while the -[p]Tp- in d(T[p]TpT) is predominantly C1′-exo (88%) but has a minor contribution from C2′-exo (12%). In the exocyclic region, a qualitative comparison of the proton-coupled ^{31}P data for d(T[p]T) (not shown) with TpD and DpT (Figure 4) indicates simliar patterns suggesting a resemblance of back-

bone torsion angles. Finally, inspection of the rotamer distributions (Table VIII) internal to the photodimer such as T[p]- ϵ(C3′–O3′), -[p]T γ(C5′–C4′), and -[p]T β(O5′–C5′) reveals similar proportions with analogous bonds in the trimers although actual values may be slightly different. A variety of NMR spectral characteristics of the photodimer nucleotides in TpDpT such as the J_{66} value, furanose and rotamer distributions, and proton-coupled ^{31}P NMR pattern (not shown) also show a high degree of similarity with the analogous moieties in d(T[p]T), TpD, and DpT. Therefore, the cis-syn photodimer in the trimers and tetramers retains the conformational properties observed in T[p]T.

Although the adjacent thymine nucleotide in either TpD or DpT has little influence on the internal structure of the photodimer, the conformational properties of some bonds and moieties neighboring the photodimer are affected in the longer oligomers. In a qualitative sense, the ^{31}P data (Table I) indicate (1) the effect of photodimerization on the internal phosphate, -[p]-, is slightly diminished with the addition of nucleotides to either the 3′ or 5′ side, (2) the effect of photodimer formation on the adjacent phosphate (e.g., Tp- or -pT) increases as nucleotides are added to either side, (3) the effect of dimerization is lost at the second nearest nucleotide, (4) the resonance position of the adjacent 5′-phosphate (Tp-) is shifted farther downfield than that of the 3′-phosphate (-pT), and (5) the proton-coupled spectra (Figure 4) for the adjacent phosphodiesters have different coupling patterns. The last two features suggest that the photodimer induces different conformational distortions in the 3′ and 5′ directions, with the effect appearing qualitatively larger on the 5′ side. Phosphodiester conformations that have more photodimer-induced distortion (e.g., Tp-) also exhibit smaller temperature-dependent ($\Delta\delta$) positions, indicating a reduced probability for additional thermally induced distortion.

A more quantitative treatment of conformational properties of the phosphodiester regions adjacent to the photodimer can be made by expressing the appropriate $J_{H,H}$, $J_{H,P}$, and $J_{C,P}$ values in terms of rotamer distributions. The most complete set of data for such a study utilizes d(TpTpT), TpD, and DpT since the unrefined ^{1}H NMR analysis of the unmodified tetramer and TpDpT limits its use here. A comparison of the rotamer distributions (Table VIII) on the 3′ side of the photodimer in d(T[p]TpT) reveals that -[p]Tp- ϵ(C3′–O3′), -pT β(O5′–C5′), and γ(C5′–C4′) are essentially unchanged from the unmodified trimer. By contrast, alterations in rotamer distribution are observed on the 5′ side of the photodimer. In the case of d(TpT[p]T), the Tp- ϵ(C3′–O3′) undergoes a 10% reduction of its trans rotamer while γ(C5′–C4′) of -pT[p]- experiences a major change in distribution from 0.83:0.11:0.05 to 0.57:0.27:0.16 upon photodimerization. The remaining exocyclic bond on the 5′ side, -pT[p]- β(O5′–C5′), retains a conformation similar to that in d(TpTpT). The Tp- ϵ(C3′–O3′) of TpDpT is observed to undergo a 20% reduction in the gauche$^-$ and trans populations to a nonclassical rotamer. These observations mean that a major destabilization of the gauche$^+$ rotamer in γ(C5′–C4′) and a minor alteration of the trans rotamer in ϵ(C3′–O3′) occur on the 5′ side of the photodimer. The alterations in these bonds may ultimately be responsible for the larger deshielding of the Tp- phosphorus resonance.

The alterations in rotamer distributions of Tp- γ(C5′–C4′) and ϵ(C3′–O3′) in addition to the unusual dT[p]- γ(C5′–C4′) value (295.5°) reported in the X-ray study of d(T[p]T) cyanoethyl ester suggests that an interpretation of these bonds in rigid angular terms is required in spite of the fact that they are expected to rotate freely. The best combination of angles for -pT[p]- γ(C5′–C4′) is 237 ± 4° (Table IX) which agrees quite well with that reported for dT[p]- γ(C5′–C4′) (240 ± 3°). The classical combination of dihedral angles (71°, 43°) for this bond may be discounted since the deviation is quite large (14°) and the distributions reveal a significant change from a highly gauche$^+$ rotamer. For Tp- ϵ(C3′–O3′), the calculated rigid angle falls into two groups: 126–143° and 205–235°. The former range can be eliminated because of its nonclassical domain, thereby leaving the best combination as the conformer in the trans class (average = 222 ± 12°).

Analysis of trimer proton–proton coupling constants reveals the effect of cis-syn photodimerization on neighboring furanose conformations (Table VII). On the one hand, the Tp- furanose moiety in unmodified d(TpTpT) and d(TpT[p]T) retains an identical distribution, 75 ± 1% C2′-endo type ↔ 25 ± 1% C3′-endo type. On the other hand, the -pT sugar is altered slightly from d(TpTpT) (61% C2′-endo type ↔ 39% C3′-endo) to d(T[p]TpT) (73% C2′-endo type ↔ 27% C2′-exo type). In the case of TpDpT, only minor changes occur for the Tp- portion. The conformational analysis of -pT in TpDpT is not performed due to the chemical shift degeneracy of H2′ and H2″, which yields only averaged $J_{1'2'}$ and $J_{1'2''}$, and $J_{2',3'}$ and $J_{2''3'}$, values.

In summary, the identification of cis-syn cyclobutane-type photodimers in various oligothymidylates is based collectively on the proton, carbon, and phosphorus NMR spectral characteristics that are common with the *cis-syn*-d(T[p]T) photodimers studied by Hruska et al. (1975) and Rycyna and Alderfer (1985).

The reported furanose distributions, exocyclic bond rotamer distributions, and rigid-angle evaluations for DpT, TpD, and TpDpT indicate different conformational parameters in the thymine nucleotides adjacent to the cis-syn photodimer. These conclusions corroborate with the results of the investigation of d(GCGTTGCG)·d(CGCAACGC) containing -T[p]T- (Kemmink et al., 1987). They report that an NOE was not found between T5(H6) and G6(H1′), which qualitatively indicates a substantial change in the structure on the 5′ side of the photodimers.

The origin of intrastrand distortion on the 5′ side (Tp-) of the photodimer can be understood by considering a conformational change involved in forming the *cis-syn*-d(T[p]T). The proton NMR (Hruska et al., 1975, 1985) and ^{13}C NMR (Rycyna & Alderfer, 1985) investigations of d(T[p]T) and, most importantly, the X-ray diffraction study of *cis-syn*-d(T-[p]T) cyanoethyl ester (Cadet et al., 1985) indicate the glycosyl conformation in dT[p]- changes from the anti to the syn range; the same bond in -[p]dT remains an anti-type conformer. A change in the -pT[p]- glycosyl bond from anti to syn probably initiates steric interactions with the adjacent Tp-, thereby inducing distortion in its conformation which is compensated by changes in γ(C5′–C4′) and ϵ(C3′–O3′). On the 3′ side of the photodimer, a minimal compensation in exocyclic angles is necessary since χ(C1′–N1) in -[p]dT remains an anti conformer. The range of extended distortion induced by the photodimer in longer thymine oligomers and polymers is currently under investigation. Preliminary results (Rycyna & Alderfer, 1986) indicate intrastrand alterations do not extend past the first nearest neighbor from the photodimer.

ACKNOWLEDGMENTS

We thank Dr. Harold C. Box for the use of his preparative HPLC facility, Peter Demou at the Chemical Instrumentation Center, Yale University, and Dr. Alex D. Bain and Dr. Charles Roger at Bruker Spectrospin (Canada) Ltd., Milton, Ontario, for recording the 500-MHz proton NMR data, and Dr. A.

Bothner-By at the NMR Facility for Biomedical Studies, Carnegie-Mellon Institute, for providing the ability to record the 600-MHz ^1H NMR spectra.

Registry No. d(TpT), 1969-54-6; d(TpTpT), 2640-26-8; d(TpTpTpT), 2476-57-5; d(TpT[p]T), 113507-39-4; d(T[p]TpT), 113490-63-4; d(TpTpT[p]T), 113490-64-5; d(TpT[p]TpT), 113564-26-4; d(T[p]TpTpT), 113490-65-6; d(T[p]TpT[p]T), 113507-40-7; acetone, 67-64-1.

REFERENCES

Alderfer, J. L., & Ts'o, P. O. P. (1977) *Biochemistry 16*, 2410–2416.

Alderfer, J. L., Lilga, K. T., French, J. B., & Box, H. C. (1984) *Chem.-Biol. Interact. 48*, 69–80.

Altona, C., & Sundaralingam, M. (1973) *J. Am. Chem. Soc. 95*, 2333–2344.

Bollum, F. J., & Setlow, R. B. (1963) *Biochim. Biophys. Acta 68*, 599–607.

Cadet, J., Voituriez, L., Hruska, F. E., & Grand, A. (1985) *Biopolymers 24*, 897–903.

Chan, G. L., Doetsch, P. W., & Haseltine, W. A. (1985) *Biochemistry 24*, 5723–5728.

Cheng, D. M., & Sarma, R. H. (1977) *J. Am. Chem. Soc. 99*, 7333–7348.

Davies, D. B., & Danyluk, S. S. (1974) *Biochemistry 13*, 4417–4434.

Fisher, G., & Johns, H. E. (1976) in *Photochemistry and Photobiology of Nucleic Acids* (Wang, S., Ed.) Vol. 1, pp 226–289, Academic, New York.

Giessner-Prette, C., & Pullman, B. (1977) *J. Theor. Biol. 65*, 171–188.

Gorenstein, D. G. (1978) in *Nuclear Magnetic Resonance Spectroscopy in Molecular Biology* (Pullman, B., Ed.) pp 1–15, Reidel, Dordrecht, Holland.

Greenstock, C. L., & Johns, H. E. (1968) *Biochem. Biophys. Res. Commun. 30*, 21–27.

Hall, R. K., & Larcom, L. L. (1982) *Photochem. Photobiol. 36*, 429–432.

Hart, R. W., Setlow, R. B., & Woodhead, A. D. (1977) *Proc. Natl. Acad. Sci. U.S.A. 74*, 5574–5578.

Hruska, F. E., Wood, D., Ogilvie, K., & Charlton, J. (1975) *Can. J. Chem. 53*, 1193–1203.

Hruska, F. E., Berger, M., Cadet, J., & Remin, M. (1985) *Can. J. Chem. 63*, 15–23.

Hutchinson, F. (1966) *Cancer Res. 26*, 2045.

Kan, L. S., Cheng, D. M., & Cadet, J. (1982) *J. Magn. Reson. 48*, 86–96.

Kemmink, J., Boelens, R., Koning, T., Koptein, R., von der Marel, G., & van Boom, J. (1987) *Eur. J. Biochem. 162*, 37–43.

Kucan, Z., Wait, H. P., & Chambers, R. W. (1972) *Biochemistry 11*, 3290–3295.

Lankhorst, P. P., Haasnoot, C. A. G., Erklens, C., & Altona, C. (1984) *J. Biomol. Struct. Dyn. 1*, 1387–1405.

Liu, F. T., & Yang, N. C. (1978) *Biochemistry 17*, 4865–4876.

Radman, M., Villani, G., Boiteux, S., Kinsella, A. R., Glickman, B. W., & Spadari, S. (1977) *Cold Spring Harbor Symp. Quant. Biol. 43*, 937–946.

Remin, M., & Shugar, D. (1972) *Biochem. Biophys. Res. Commun. 48*, 636–642.

Rothman, R. J., & Setlow, R. B. (1979) *Photochem. Photobiol. 29*, 57–61.

Rycyna, R. E., & Alderfer, J. L. (1985) *Nucleic Acids Res. 13*, 5949–5963.

Rycyna, R. E., & Alderfer, J. L. (1986) *Biophys. J. 49*, 128a.

Sauerbier, W. (1976) *Adv. Radiat. Biol. 6*, 49–106.

Schweizer, M. P., Banta, E. B., Witkowski, J. T., & Robins, R. K. (1973) *J. Am. Chem. Soc. 95*, 3770–3778.

Setlow, J. K. (1966) *Curr. Top. Radiat. Res. 2*, 195.

Setlow, R. B., Carrier, W. L., & Bollum, F. J. (1964) *Biochim. Biophys. Acta 91*, 446–461.

Suzuki, F., Han, A., Lanker, G. R., Utsumi, H., & Elkind, M. M. (1981) *Cancer Res. 41*, 4916–4924.

Uesugi, S., & Ikehara, M. (1977) *J. Am. Chem. Soc. 99*, 3250–3253.

Varghese, A. J. (1972) *Photophysiology 7*, 207–274.

Wang, S. Y., Ed. (1976) *Photochemistry and Photobiology of Nucleic Acids*, Vols. 1 and 2, Academic, New York.